

A Novel Timing Synchronization Method for MIMO-OFDM Systems

Ali Rachini

Fabienne Nouvel

Ali Beydoun and Bilal Beydoun

IETR - INSA de Rennes, France

GET/UL - Lebanese University

Email: Ali.Rachini@ul.edu.lb fabienne.nouvel@insa-rennes.fr

IETR - INSA de Rennes

Rennes, France

GET/UL - Lebanese University

Hadath, Lebanon

bilbey@ul.edu.lb

beydoul@yahoo.fr

Abstract—To increase the throughput of transmission systems, MIMO-OFDM technology enables better transmission rate and improves the reception. The synchronization between the transmitter and the receiver has become a big challenge. A bad timing synchronization causes the loss of a lot of information in a MIMO-OFDM system. In this paper, a novel timing synchronization method is proposed for a MIMO-OFDM systems with N_t transmit antennas and N_r receive antennas. The proposed method is based on transmit an orthogonal CAZAC sequences over different transmit antennas [1]. Simulations results show that the proposed solution presents a good performance at a low SNR (Signal to Noise Ratio) in AWGN and multipath fading Rayleigh channels, where Doppler Effect is not considered for current simulations. Furthermore, this method can be implemented for MIMO-OFDM system up to 8×8 as well. In the proposed method, the coarse and fine timing synchronization are done at the same time at each receive antenna due to the different training sequences transmitted over different transmit antennas.

Keywords - MIMO-OFDM system, timing synchronization, CAZAC sequences, compact preamble

I. INTRODUCTION

The world of wireless communications and mobile communication is currently at a very important crossroads in its evolution. This crossroads introduces a variety of challenges such as multi-path signal reflections, and interference. These can reduce the performance of a receiver. To address these challenges, OFDM (Orthogonal Frequency Division Multiplexing) modulation combined with MIMO (Multiple Input-Multiple Output) is proposed in 802.11n [2].

The OFDM [3] divides a frequency bandwidth into several (N_{sc}) orthogonal sub-carrier. To simply achieve orthogonal frequency multiplex, Saltzberg and Weinstein [4] have shown that the use of the FFT algorithm (Fast Fourier Transform) can easily produce the OFDM symbol carried by N_{sc} orthogonal subcarriers. The IFFT (Inverse Fast Fourier Transform) algorithm is also used to demodulate the message at the receiver. To maintain the orthogonality, the sub-carrier spacing required is $\Delta f = \frac{1}{T_s}$, where T_s is the duration of OFDM symbol. Due to this orthogonality, OFDM is more resistant to frequency selective fading than FDM (Frequency Division Multiplexing) systems. The orthogonality of frequencies is primordial to eliminate the ICI (Inter Carrier Interference). On the other hand, it should be noted that the

most important disadvantage of OFDM is probably the PAPR (Peak-to-Average Power Ratio), leading to replacing it on the up-link in LTE (Long-Term Evolution).

Otherwise, to reduce the ISI (Inter Symbol Interference) due to the multipath fading channel, OFDM technology uses a technique that consists to insert a GI (Guard Interval) [5] or CP (Cyclic Prefix) of duration T_g . The duration of CP should be greater than or equal to the maximum spread of the channel impulse response τ_{max} . The CP is usually a copy of the last portion of an OFDM symbol. Therefore, the useful part T_s of each OFDM symbol will no longer be affected by the ISI. The total duration of the OFDM symbol is $T_{tot} = T_s + T_g$.

Furthermore, MIMO is a wireless technology that uses multiple transmit antennas (N_t) and multiple receive antennas (N_r) to transmit data at the same time. Several applications, based on MIMO technology, have been proposed in various communication standards as WiFi (Wireless Fidelity), WiMax (Worldwide Interoperability for Microwave Access), HSPA+ (evolved High-Speed Packet Access), 3rd and 4th generation of mobile network and LTE. MIMO is based on two main techniques [6], [7]: Spatial Multiplexing techniques (SM) and Spatial Diversity techniques (SD).

- 1) Spatial Multiplexing technique (SM): The spatial multiplexing technique transmits independent data streams, over different antennas, in order to increase the transmission data rates in a given frequency bandwidth. MIMO systems are mainly used to increase the flow of wireless communications. Foshini et al. [8] and Telatar [9] have shown that the theoretical capacity of the MIMO channel, with N_t transmit antennas and N_r receive antennas, increases linearly with $\min(N_t, N_r)$. The channel capacity of a MIMO system is defined by the equation (1) [8], [9]:

$$C = \log_2 \left[\det \left(I_{N_r} + \frac{\rho}{N_t} H H^\dagger \right) \right] \text{bps/Hz.} \quad (1)$$

with

- N_t : Number of transmit antennas.
- N_r : Number of receive antennas.
- I_{N_r} : Identity matrix $N_r \times N_r$.
- $(\cdot)^\dagger$: Conjugate transpose.
- H : MIMO channel matrix $N_t \times N_r$.

- $\rho = \frac{P}{N_0 B}$: Signal to noise ratio (SNR).
- P : Total transmitted power.
- N_0 : Power Spectral Density (PSD).

2) Spatial Diversity technique (SD): Spatial diversity technique consists of sending the same data stream simultaneously on different transmit antennas. At the receiver, several versions of the signal are received and combined on each of the antennas. This combination reduces the attenuation of the signal and compensates the effect of fading channels. This diversity requires to make use of STC (Space-Time Codes) such as Alamouti codes [10] or trellis codes [11]. Spatial diversity has good efficiency when the MIMO sub-channels are decorrelated to each other. Furthermore, when the number of transmit antennas increases, the power of the received signal increases, thereby improving the detection of received signal.

In this paper, we will focus on spatial diversity technique using STBC (Space-Time Block Code) with Alamouti [10] encoder.

One of the main challenges for MIMO-OFDM system is the synchronization between transmitter and receiver. Two types of synchronization are necessary, the frequency and the timing synchronization. The frequency synchronization is based on the detection of the frequency offset between the transmitter and the local oscillator at the receiver [12]. The CFO (Carrier Frequency Offset) is presented due to the Doppler effect or the difference between the frequency between transmitter and receiver in MIMO-OFDM systems. In the other hand, timing synchronization is divided into two parts: the coarse timing synchronization detects the arrival of the OFDM frame and the fine timing synchronization is needed to detect the beginning of OFDM symbols on each frame. The timing synchronization is very important on each communication system and it is important to have a robust algorithm to estimate the timing synchronization in order to detect the start of each OFDM frame and symbol. In this paper, we focus on the timing synchronization in MIMO-OFDM systems.

In the literature, several synchronization approaches have been proposed for OFDM and MIMO-OFDM systems [13]–[17]. The main idea is the use of good synchronization preamble, at the transmitter, in order to detect the packet arrival, at the receiver.

In this paper, we propose a novel preamble structure for timing synchronization in MIMO-OFDM systems using CAZAC (Constant Amplitude Zero Auto-Correlation) sequences. The CAZAC sequences [18] are a class of complex-valued sequences with cyclic autocorrelation equal

to zero. The main characteristics of CAZAC sequences are their zero auto-correlation; it means that a CAZAC code is always orthogonal with its cyclic shifted versions. Furthermore, they have a constant amplitude. The main benefits of CAZAC sequences are the reduction of ISI and they avoid interferences between multiple antennas. As a result, CAZAC sequences are regarded as preamble for timing synchronization in MIMO-OFDM systems.

This paper is organized as follows. Section II briefly describes the MIMO-OFDM system structure based on STBC code. Related work are presented in Section III. Section IV introduces the criteria to select a good synchronization sequences. The proposed method and preamble structure are presented in Section V. Simulation results and conclusion are given in Sections VI and VII, respectively.

II. SYSTEM MODEL

Like any telecommunications system, MIMO-OFDM system consists of a transmitter, a channel, and a receiver. The transmitter generates OFDM symbols which are modulated using QAM (Quadrature Amplitude Modulation). The OFDM symbols are transmitted over multiple antennas using space time coding block (STBC) [10], [19]. The STBC is a technique to transmit multiple copies of a data stream across N_t transmit antennas in a MIMO system. It exploits the spatial diversity and increases the reliability of transmission. This type of code is divided into three main approaches [19]: OSTBC (Orthogonal Space-Time Block Codes), NOSTBC (Non-Orthogonal Space-Time Block Codes) and QSTBC (Quasi-Orthogonal Space-Time Block Codes). Our approach is based on the STBC using Alamouti code [10].

A. MIMO-OFDM System

Figure 1 presents a MIMO-OFDM system with N_t transmit antennas, N_r receive antennas and N_{sc} subcarriers per transmit antenna. The data block is used in order to generate the bitstream, then a serial/parallel (S-to-P) converter is used to distribute the datastream to the QAM modulator (Sub carrier mapping). This modulator maps the bit stream according to the 32-QAM modulation. The QAM symbols are then introduced into a STBC encoder. Then, we apply the IFFT to generate the OFDM symbols. A cyclic prefix block (Add CP) consist to insert a guard interval between successive OFDM symbols, which the last T_G seconds of each symbol is appended to the beginning of each OFDM symbol. The CP is used in order to minimize the ISI and it will be removed at the receiver before to the FFT. The synchronization block is used in order to insert the synchronization preamble at the beginning of each OFDM frame. Two different approaches are presented, the synchronization preamble is appended in frequency domain or in time domain. In this paper, we focus on the first approach. In [20], we proposed another method that generates the synchronization preamble in time domain.

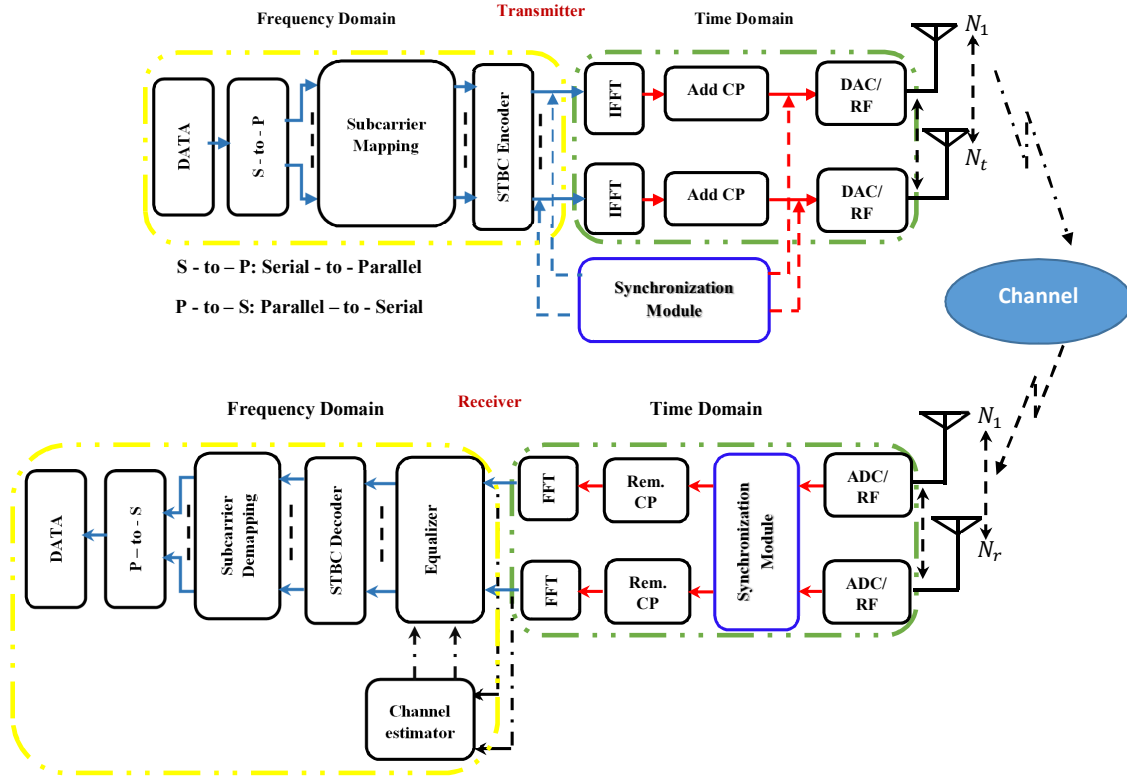


Fig. 1: Transmission system MIMO-OFDM-STBC

The transmitted signal s_i on each transmit antenna T_i is given by:

$$s_i(t) = \frac{1}{\sqrt{N_{sc}}} \sum_{k=0}^{N_{sc}-1} \Re \{ x_k e^{j \cdot 2\pi \cdot f_k \cdot t} \} \quad (2)$$

where x_k is the symbol on the frequency f_k .

The second part of MIMO-OFDM system is the receiver. The first block after the analog to digital converter (ADC) is the timing synchronization block. After a good timing synchronization, the cyclic prefix of each OFDM symbol is eliminated. The signal returns back into frequency domain thanks to FFT block. The equalization is used in order to fight the ISI problem, which is created by multipath fading channels, taking into account the channel estimation coefficients. The estimated symbols are decoded and combined by the STBC decoder. Then, a QAM demodulator is used to demodulate and recover the binary information. The parallel/serial (P-to-S) converter allows to reformatting the binary bit stream.

B. Channel Model

The transmitted signal reaches the receiver over different paths due to the multipath channel. The channel between the transmit antennas T_i and receive antenna R_j , $i \in \{1, N_t\}$ and $j \in \{1, N_r\}$, is given by:

$$H(t) = \sum_{l=1}^L H_l \delta(t - \tau_l) \quad (3)$$

where H_l are the matrix coefficients of the l^{th} path. This matrix is $N_t \times N_r$. δ is a pulse function and L is the maximum number of multipaths. H_l is given by:

$$H_l = \begin{bmatrix} h_{1,1}^l & h_{1,2}^l & \dots & h_{1,N_r}^l \\ h_{2,1}^l & h_{2,2}^l & \dots & h_{2,N_r}^l \\ \vdots & \vdots & \ddots & \vdots \\ h_{N_t,1}^l & h_{N_t,2}^l & \dots & h_{N_t,N_r}^l \end{bmatrix} \quad (4)$$

C. Received signal

The received signal r_j on each receive antenna R_j is given by:

$$r_j(t) = \sum_{i=1}^{N_t} \sum_{l=1}^L \left(h_{ij}^l(t) \cdot s_i(t) \right) + w_j(t) \quad (5)$$

where s_i is the transmitted signal on the transmit antenna T_i , w_j is the additive white Gaussian noise (AWGN) and h_{ij}^l represents the corresponding channel between T_i and R_j .

The matrix representation of the received signal is given by:

$$\begin{bmatrix} r_1 \\ r_2 \\ \vdots \\ r_{N_r} \end{bmatrix} = \begin{bmatrix} H_{1,1} & \dots & H_{1,N_r} \\ H_{2,1} & \dots & H_{2,N_r} \\ \vdots & \ddots & \vdots \\ H_{N_t,1} & \dots & H_{N_t,N_r} \end{bmatrix} \times \begin{bmatrix} s_1 \\ s_2 \\ \vdots \\ s_{N_t} \end{bmatrix} + \begin{bmatrix} w_1 \\ w_2 \\ \vdots \\ w_{N_r} \end{bmatrix} \quad (6)$$

III. RELATED WORK

In the literature, several synchronization approaches have been proposed for OFDM and MIMO-OFDM as shown in Section I. The most of the synchronization methods are preamble based.

Authors in [21] provides a method for timing and frequency synchronization for a MIMO-OFDM system using the LS (Loosely Synchronous) codes to detect the beginning of each received frame. LS codes have a good autocorrelation and cross-correlation functions within certain vicinity of the zero shifts. In this method, the synchronization process is divided into four steps. The first step is to estimate the coarse timing synchronization and, the second step is to estimate the coarse frequency synchronization. The third step detects the OFDM symbols and estimates the channel using the LS codes, the fourth step is for the fine frequency estimation. Furthermore, the structure of preambles used in the process is relatively complex.

Authors in [22] proposed a timing synchronization method based on OVSA (Orthogonal Variable Spreading Factor). Simulations results are done using MISO (Multiple Input-Single Output) systems 2×1 . The length of each OFDM symbol is 256, and the length of the CP is 32. A synchronization preamble is appended at the beginning of each OFDM frame, this preamble has the same length as the CP. For MISO-OFDM systems 2×1 , the timing acquisition probability is 1 for $SNR \geq -5 \text{ dB}$. The synchronization preamble for this method is appended in the time domain, this is the main drawback of this method. With such implementation, authors need an extra block to insert the preamble, while, in frequency domain we do not need any extra block thanks to IFFT.

Based on our proposed approach, a compact preamble design for synchronization in distributed MIMO-OFDM systems has been proposed in [23]. The authors have designed training symbols based on exclusive subband, where different adjacent subbands are spaced by guard bands to reduce their mutual interference. In [23], authors propose a compact preamble structure that has the same length as an OFDM symbol. This preamble, based on CAZAC sequences, is carried by a different subbands. The simulation results shown that for a MISO-OFDM (3×1), the acquisition probability for timing synchronization is 70% for an $SNR = 5 \text{ dB}$. In this work, we compare the simulation results of our proposed [1] with those of the method proposed

by Chin-Liang et al [23].

The proposed method in [23] has several limitations such as the complexity of the structures to generate the synchronization preambles for a large number of transmit antennas. In [23], when the number of transmit antennas increases, the size of sub-bands should be reduced to take into account all transmit antennas. Therefore, at the receiver, the probability of synchronization decreases due to the length of synchronization sequence.

IV. SELECTION CRITERIA FOR SYNCHRONIZATION SEQUENCES

Most of timing synchronization methods are based on preamble approach. They consist in sending a synchronization preamble at the beginning of each OFDM frame. The main characteristic of synchronization preamble is to have good autocorrelation and cross-correlation properties in order to detect a correlation peak as closed as possible to a Dirac pulse. On the other hand, the synchronization preambles should be orthogonal to eliminate the interferences between preambles at simultaneous transmissions in MIMO systems. The main sequences used in the state of art are listed below.

A. Gold sequences

Gold sequences have been proposed by Robert Gold in 1967 [24]. These sequences are constructed by two PN (Pseudorandom Noise) sequences of the same length. The XOR (\oplus) is the operation to generate Gold sequences. Let x and y be two PN maximum length sequences of the length $L_C = 2^l - 1$. The set $S_{gold}(x, y)$ of Gold sequences is given by:

$$S_{gold}(x, y) = \{x, y, x \oplus y, x \oplus T^{-1}y, \dots, x \oplus T^{-(L_C-1)}y\} \quad (7)$$

where T^{-p} is an operator of cyclic shifts of p values to the left.

The cross-correlation peak of some periodic Gold sequences take one of the three possible values -1 , $-t(l)$ or $t(l) - 2$, where $t(l)$ is given by:

$$t(l) = \begin{cases} 2^{(l+2)/2} + 1 & \text{if } l \text{ is even} \\ 2^{(l+1)/2} + 1 & \text{if } l \text{ is odd} \end{cases} \quad (8)$$

The disadvantage of Gold sequences is inter-code interference due to high cross-correlation. In this paper, the synchronization preamble is appended at the beginning of each OFDM frame and is transmitted aperiodic. Therefore, the autocorrelation and cross-correlation functions of aperiodic Gold sequences are shown in Figure 2 where index represents indices at which the correlation was estimated.

B. Walsh-Hadamard code

Walsh-Hadamard code are built recursively from a 2×2 Hadamard's matrix [25]. These codes are orthogonal and bipolar, where the Hadamard's matrix is given by:

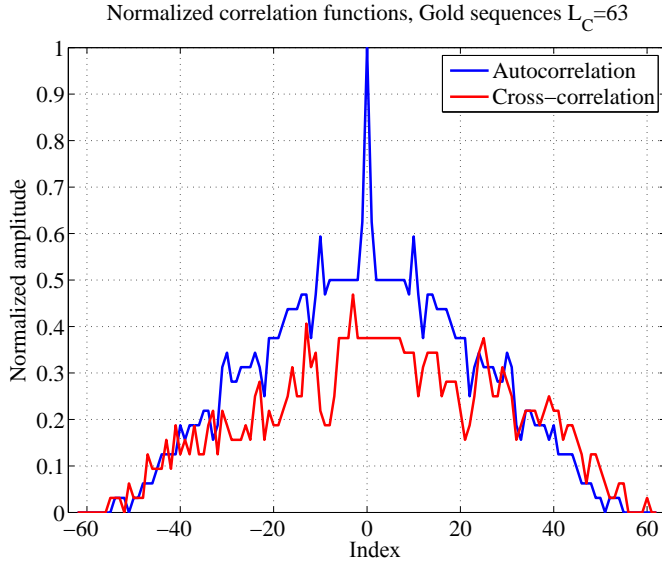


Fig. 2: Autocorrelation and cross-correlation of Gold sequence, $L_C = 63$

$$H_2 = \begin{bmatrix} 1 & 1 \\ 1 & -1 \end{bmatrix}, \dots, H_{2^k} = \begin{bmatrix} H_{2^{k-1}} & H_{2^{k-1}} \\ H_{2^{k-1}} & -H_{2^{k-1}} \end{bmatrix} \\ = H_2 \otimes H_{2^{k-1}} \text{ for } 2 \leq k \in \mathbb{N} \quad (9)$$

where \otimes denotes the Kronecker product.

An Hadamard matrix H_n satisfies the following property:

$$H_n \cdot H_n^T = nI_n$$

where H_n^T is the conjugate transpose of H_n and I_n is a $n \times n$ identity matrix. The autocorrelation and cross-correlation functions of Hadamard sequences are shown in Figure 3.

C. CAZAC sequences

The CAZAC (Constant Amplitude Zero Auto-Correlation) sequences [26] are a class of complex-valued sequences with cyclic autocorrelation equal to zero. CAZAC sequences are characterized by their constant amplitude and their correlation function. The cross-correlation function between two different CAZAC sequences is near to zero and the autocorrelation function is as δ . Let $x_u(k)$ be a CAZAC sequence of length L_C , $x_u(k)$ is given in equation (10):

$$C(k) = \begin{cases} e^{j\left(\frac{\pi M k(k+1)}{L_C}\right)} & \text{if } L_C \text{ is odd} \\ e^{j\left(\frac{\pi M k^2}{L_C}\right)} & \text{if } L_C \text{ is even} \end{cases} \quad (10)$$

where $L_C = 2^n$ is the length of the CAZAC sequence, $n \in \mathbb{N}$, $M \in \mathbb{N}$ is a prime number with L_C and $k \in \{0, L_C - 1\}$ is the index of the sample.

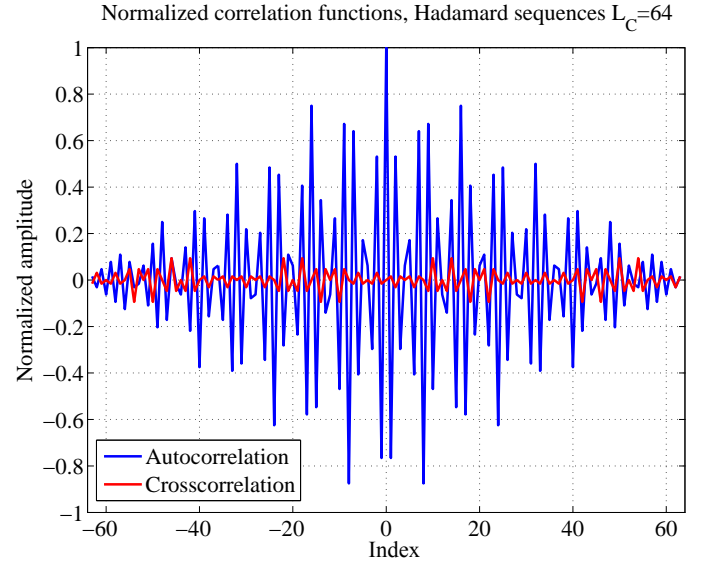


Fig. 3: Autocorrelation and cross-correlation of Hadamard sequence, $L_C = 64$

Let $c(m)$ be the corresponding of $C(k)$ in the time domain after the IFFT. It should be noted that $c(m)$ is also a CAZAC sequence of length L_C [27]. This sequence $c(m)$ is given by the equation (11):

$$c(m) = \frac{1}{L_C} \sum_{k=0}^{L_C-1} C(k) \cdot e^{j\left(\frac{2\pi}{L_C}\right)mk}, m \in [0, L_C - 1] \quad (11)$$

The autocorrelation and cross-correlation functions of CAZAC sequences are shown in Figure 4.

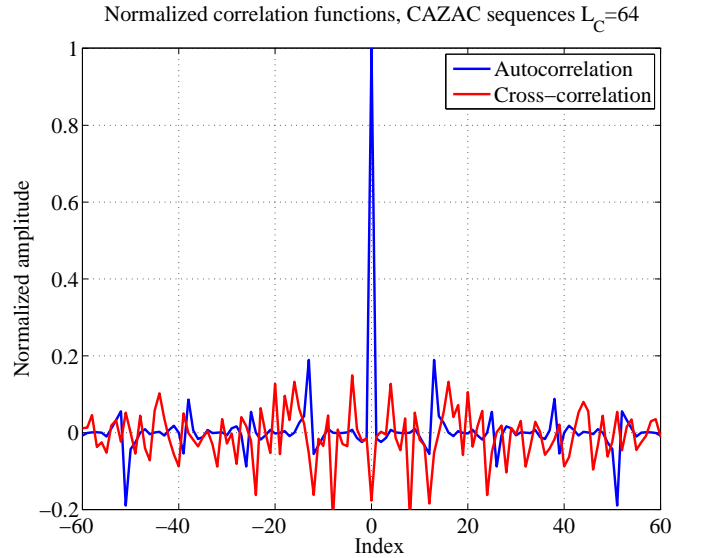


Fig. 4: Autocorrelation and cross-correlation of CAZAC sequence, $L_C = 64$

D. Selection criteria

Both Gold and Hadamard sequences have good correlation functions, but Gold sequences have a high value for their cross-correlation function, while for some Hadamard sequences, the autocorrelation function has secondary correlation peaks. In the other hand, and as shown in Figure 4, CAZAC sequences have a good autocorrelation and cross-correlation functions. In this paper, our work was focused on the use of CAZAC sequence as synchronization sequences in the synchronization preamble with different structures.

V. PROPOSED METHOD FOR TIMING SYNCHRONIZATION

In this section, we present our timing synchronization method based on CAZAC sequences. We define, in this section, C as a CAZAC sequence of length L_C , where:

$$L_C = L_{FFT}/2 \quad (12)$$

L_{FFT} is the size of the FFT and $-C^*$ is the minus conjugate of C of length L_C . This approach is based into two structures.

A. First preamble structure

The proposed timing synchronization structure, in this section, relies on sending a preamble structure performed in the frequency domain, as shown in Figure 5.



Fig. 5: General preamble structure in frequency domain for the first structure

In Figure 5, each preamble contains a CAZAC (C) sequence mapped on the odd subcarrier, in frequency domain, and the $-C^*$ is mapped on the even subcarrier. Let $X_u^i(k)$ be the preamble that appended at the beginning of each OFDM frame in frequency domain on the i^{th} transmit antenna. This preamble can be given by the following equation:

$$X_u^i(k) = \begin{cases} C^i\left(\frac{k}{2}\right) & \text{if } k \bmod 2 = 0 \\ -C^{i*}\left(\frac{k-1}{2}\right) & \text{if } k \bmod 2 \neq 0 \end{cases} \quad (13)$$

where $k \in \{0, L_{FFT} - 1\}$ and $L_{FFT} = 2.L_C$.

Figure 6 presents the real and the imaginary parts of the synchronization preamble in time domain. The combination of a CAZAC sequence C with $-C^*$ gives a time-domain complex envelope form that have a good autocorrelation and cross-correlation functions. This combination does not destroy the orthogonality between subcarriers, and it retains

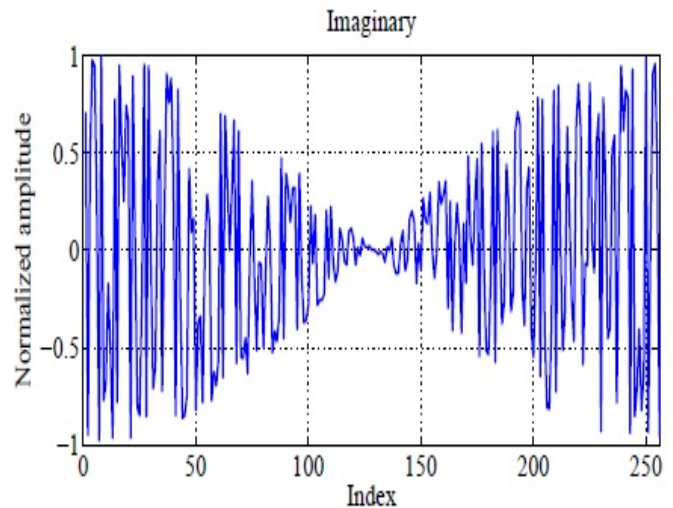
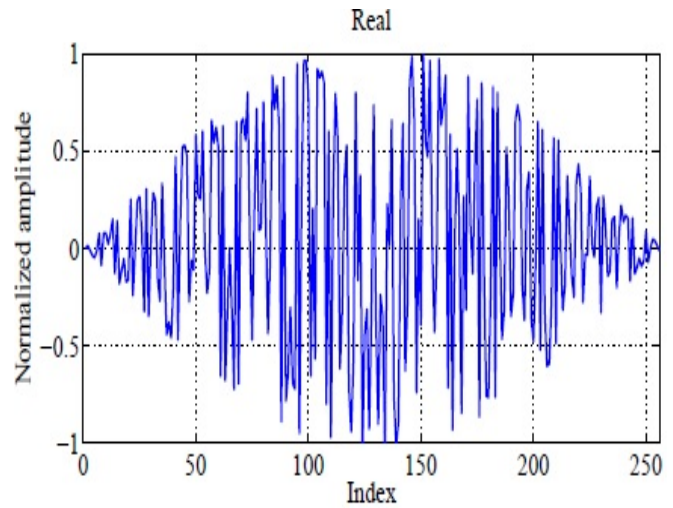


Fig. 6: Real and imaginary parts of the first preamble structure in time domain

the orthogonality between different preambles over different transmit antennas.

Figure 7 presents the autocorrelation and the cross-correlation of the proposed preamble in time domain. This preamble shows a good correlation function in order to detect the timing synchronization peak.

Figure 8 represents different CAZAC sequences transmitted over different transmit antennas. The term C_k^i is the sample of the CAZAC sequence carried by the k^{th} subcarrier and transmitted by the transmitting antenna T_i . The proposed method can be applied regardless of the number of transmit or receive antennas.

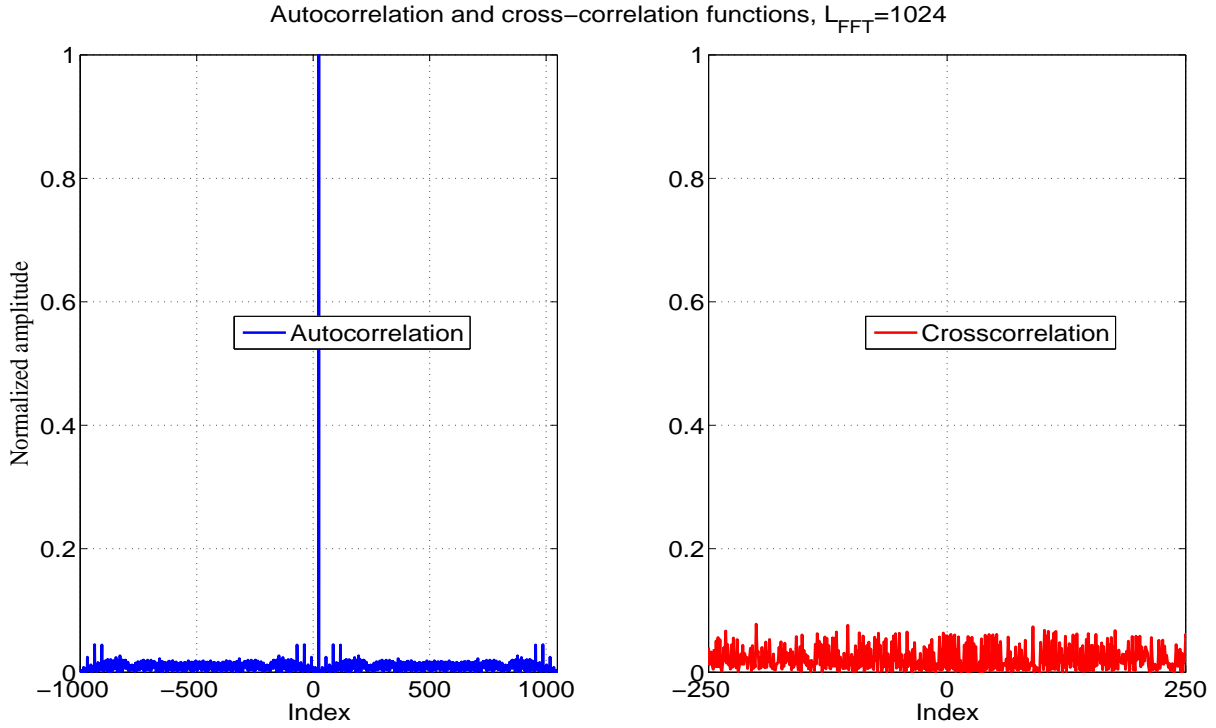


Fig. 7: Autocorrelation and cross-correlation functions of the first preamble structure ($L_{FFT} = 1024$)

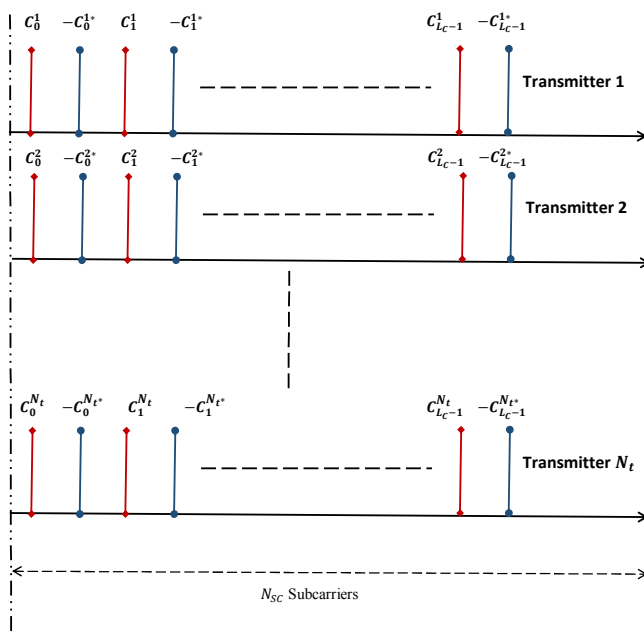


Fig. 8: First preamble structure in frequency domain over different transmit antennas

B. Second preamble structure

The second preamble structure is based on the first preamble structure, where the preamble is divided into two parts of

length L_C each one. The first part contains a complete CAZAC sequence C , where the second part contains the minus conjugate of C denoted $-C^*$. Different CAZAC sequences are transmitted over different transmit antennas. This preamble structure is presented in Figure 9 in frequency domain.

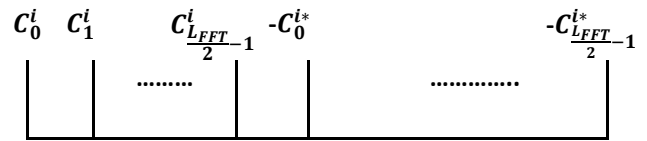


Fig. 9: General preamble structure in frequency domain for the second structure

The autocorrelation and cross-correlation functions of this preamble in time domain are presented in Figure 10. The autocorrelation function of this preamble has a secondary peak at 30% of the normalized autocorrelation peak.

Let X_u^i be the preamble sent on the i^{th} transmit antenna, the equation of this preamble in frequency domain is given by:

$$X_u^i(k) = \begin{cases} C^i(k) & \text{if } 0 \leq k \leq L_C - 1 \\ -C^{i*}(k - L_C) & \text{if } L_C \leq k \leq L_{FFT} - 1 \end{cases} \quad (14)$$

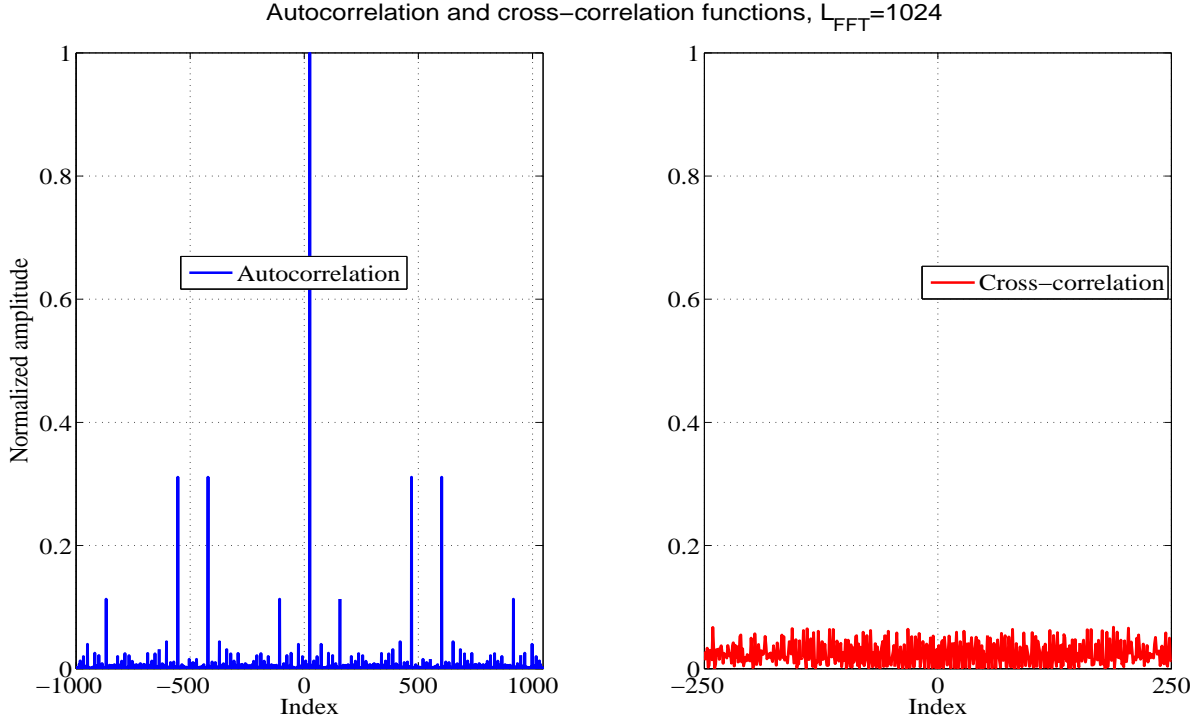


Fig. 10: Autocorrelation and cross-correlation functions of the second preamble structure ($L_{FFT} = 1024$)

VI. SIMULATIONS RESULTS

The simulations have been done, in both AWGN channel and multipaths fading channel, to evaluate the performance of our proposed preamble against previous proposed preamble.

A. Simulation parameters

A SISO-OFDM (Single Input-Single Output) and MIMO-OFDM systems up to 8×8 transmit and receive antennas were simulated. An OFDM system with 512 and 1024 subcarriers ($L_{FFT} = 512, L_{FFT} = 1024$ resp.) was considered in Rayleigh multipath fading channel with 6 paths sample-spaced with T_s (Sampling Time), suggested by the IEEE 802.11 Working Group [28]. The simulation parameters are summarized in the following Tables I and II.

TABLE I: Simulation parameters

Simulation Parameters	Value
MIMO	up to 8×8
FFT/IFFT Length	1024 & 512
Cyclic Prefix Length	$L_{FFT}/4$
Channel Type	Multi-path Rayleigh and AWGN channel
Sequences	CAZAC
Length of orthogonal code L_C	$L_{FFT}/2$
Number of synchronization symbol	1
Number of channel taps between different antennas	6
SNR over all the OFDM Frame	from 0dB to 25dB

TABLE II: The average power profile of the multipath Rayleigh channel model

Propagation delay between different multipath	$[0.T_s, 1.T_s, 2.T_s, 3.T_s, 4.T_s, 5.T_s]$
The power of each multipath	$[0.8111, 0.1532, 0.0289, 0.0055, 0.0010, 0.0002]$

B. Timing synchronization

In order to detect the timing synchronization peak, a correlation function \mathcal{R}_{r_j, seq_j} between the received signal r_j [equation (5)] and the local sequence seq_j at the receive antenna R_j is applied in time domain. Due to the distribution of CAZAC sequence C and $-C^*$ in each preamble, the correlation between received signal and the local sequence may give a high peak's value. The correlation function is calculated as:

$$\mathcal{R}_{r_j, seq_j}(n) = \sum_{n=1}^L [r_j(n) * seq_j(n - \tau)] \quad (15)$$

where n is the index of the sample.

By correlating the received signal r_j with a local sequence seq_j at each receive antenna R_j , a timing synchronization estimate ($\hat{i}nd_n$) is given by:

$$\hat{i}nd_n = \underset{n}{\operatorname{argmax}} \{ \|\mathcal{R}_{r_j, seq_j}(n)\| \} \quad (16)$$

The $\hat{i}nd_n$ is the timing estimate where n is considered as the coarse timing synchronization point. By shifting the FFT

window, we can find the fine timing synchronization or the beginning of the OFDM symbols on each frame.

C. Simulation results for the first preamble structure

The first preamble structure, presented in Section V, were simulated using the simulation parameters in Tables I and II. The probability of successful timing frame synchronization P_{SYNC} is evaluated in Figures 11 and 12. They show the acquisition probability for different OFDM systems (SISO-OFDM, MIMO-OFDM up to 8×8), using CAZAC sequences. The lengths of preamble are 1024 and 512, respectively ($L_{FFT} = 1024$, $L_{FFT} = 512$ resp.).

Figure 11 shows that the system has achieved a synchronization probability over 95% at an $SNR = -5dB$ for both SISO-OFDM and MIMO-OFDM 2×2 systems. For a MIMO-OFDM 4×4 system the $P_{SYNC} > 97\%$ at an $SNR = 0dB$. On the other hand, for MIMO-OFDM 8×8 system, the acquisition probability P_{SYNC} reaches 90% at an $SNR = 0dB$.

In Figure 12 and for $L_{FFT} = 512$, it should be mentioned that the acquisition probability P_{SYNC} is greater than 99% for both SISO-OFDM and MIMO-OFDM 2×2 systems at an $SNR = -5dB$, and $P_{SYNC} > 90\%$ for MIMO-OFDM 4×4 system at an $SNR = 0dB$. For MIMO-OFDM 8×8 system the P_{SYNC} reaches 80% at an $SNR = 3dB$.

For MIMO-OFDM systems, the limitations of all timing synchronization methods, are the number of transmit antennas and the length of the synchronization preamble.

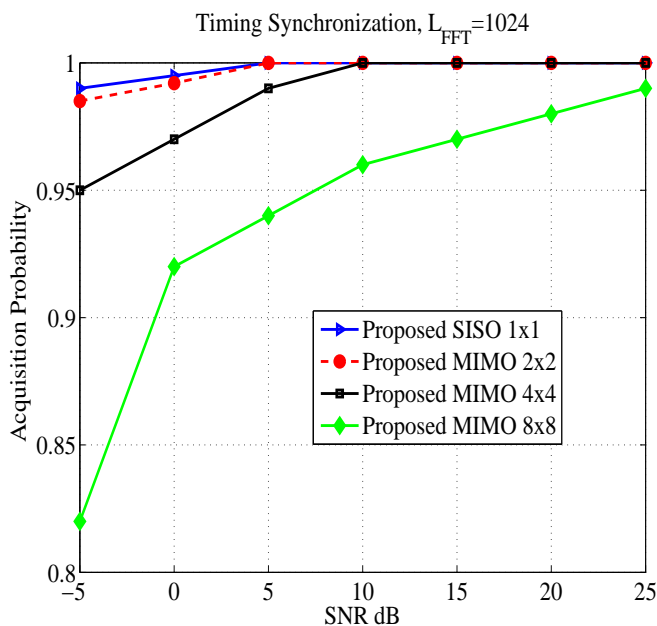


Fig. 11: Timing synchronization performance of the first proposed approach ($L_{FFT} = 1024$)

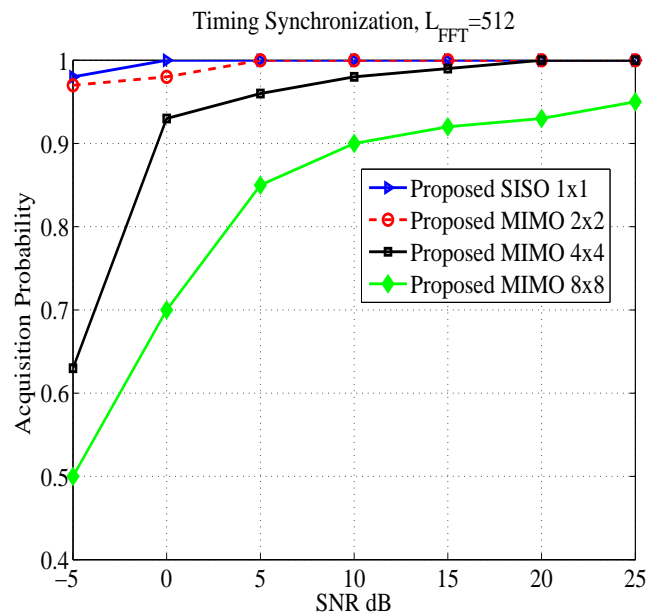


Fig. 12: Timing synchronization performance of the first proposed approach ($L_{FFT} = 512$)

The simulation results of our proposed method (Figure 11) shows a good performance in terms of timing synchronization acquisition probability for MIMO-OFDM system up to 8×8 , with a preamble length equal to 1024. A degradation of performances in term of P_{SYNC} (Figure 12) is observed when the length of preamble is smaller than the length used in Figure 11. The degradations of P_{SYNC} , for a large number of transmit antennas, are due to the length of the synchronization preamble. Otherwise, at the receiver, as the length of the preamble is longer then the probability of timing synchronization is higher.

In Figure 13, we compared the performance between our proposed approach and the synchronization scheme in [23]. Based on simulation parameters presented in Tables I and II, our proposed method has a good performance against those obtained by [23]. Furthermore, this figure shows that the acquisition probability P_{SYNC} of our proposed method is greater than 90% for a $SNR > 3dB$ for both MIMO-OFDM 2×2 and 3×3 systems, while the method proposed in [23], shows that the acquisition probability is between 50% and 75% for a $SNR > 3dB$. On the other hand, and for both MIMO-OFDM 2×2 and 3×3 systems, our method presents a perfect timing synchronization for a $SNR > 10dB$.

D. Simulation results for the second preamble structure

This section presents the simulation results for the second preamble structure presented in Section V. This simulation are performed using the simulation parameters in Tables I and II.

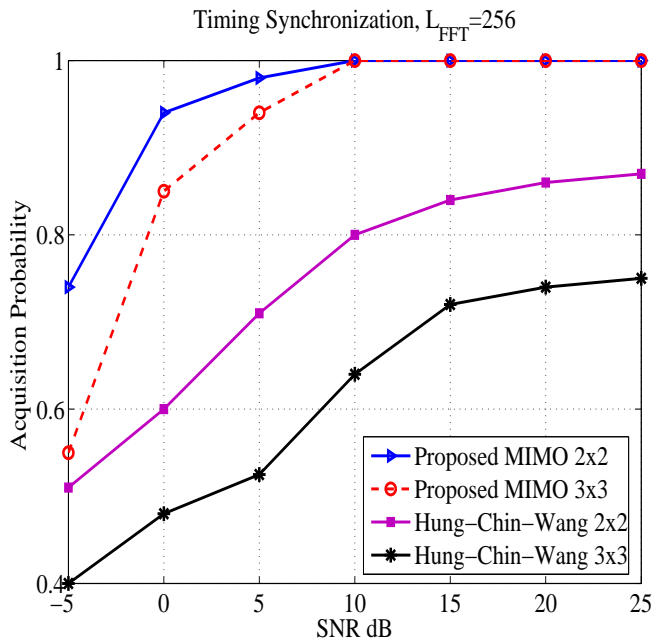


Fig. 13: Comparisons between the first proposed approach and subband-based preamble proposed in [23]

The timing acquisition probability P_{SYNC} for different size of FFT ($L_{FFT} = 1024$ and $L_{FFT} = 512$) is shown in Figures 14 and 15, respectively.

Figure 14 shows that for a $L_{FFT} = 1024$ and a $SNR \geq -5$ dB, the acquisition probability P_{SYNC} is greater than 95% for both SISO-OFDM and MIMO-OFDM 2×2 systems. Otherwise, the synchronization probability is perfect from a $SNR \geq 5$ dB for the same systems. On the other hand, for a MIMO-OFDM 4×4 system the P_{SYNC} is greater than 96% for a $SNR \geq 0$ dB, and its equal to 1 for a $SNR \geq 15$ dB. Therefore, the acquisition probability for MIMO-OFDM 8×8 system, reaches 90% for an $SNR > 2$ dB.

In Figure 15, the simulation results are performed with an $L_{FFT} = 512$. This figure shows that the acquisition probability P_{SYNC} is greater than 99% for both SISO-OFDM and MIMO-OFDM 2×2 systems at an $SNR = 0$ dB, and $P_{SYNC} > 90\%$ for MIMO-OFDM 4×4 system at an $SNR = 0$ dB. For MIMO-OFDM 8×8 system the P_{SYNC} reaches 90% at an $SNR = 13$ dB.

Other simulations are performed to compare our second proposed approach with the method proposed in [23], using the same simulation parameters of Tables I and II. Results are shown in Figure 16. In this figure, the size of the preamble is $L_{FFT} = 256$. As shown in this figure, the timing synchronization acquisition probability for our proposed approach is better than the proposed method in [23].

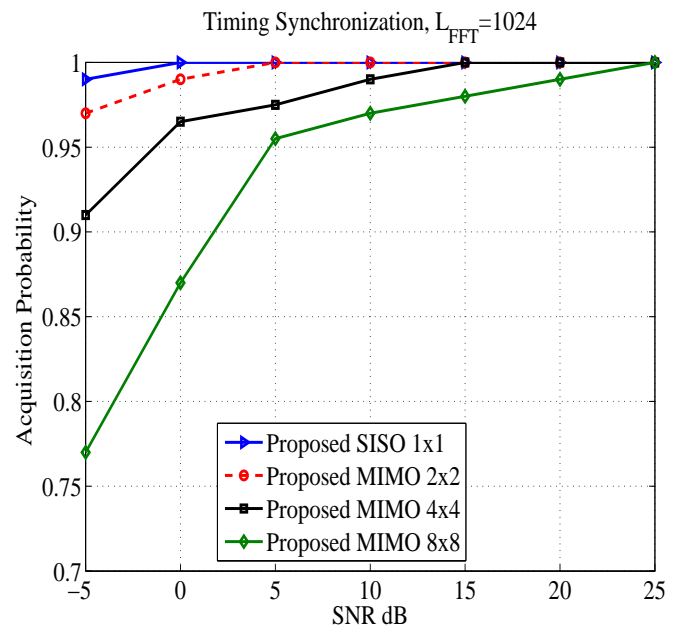


Fig. 14: Timing synchronization performance of the second proposed approach ($L_{FFT} = 1024$)

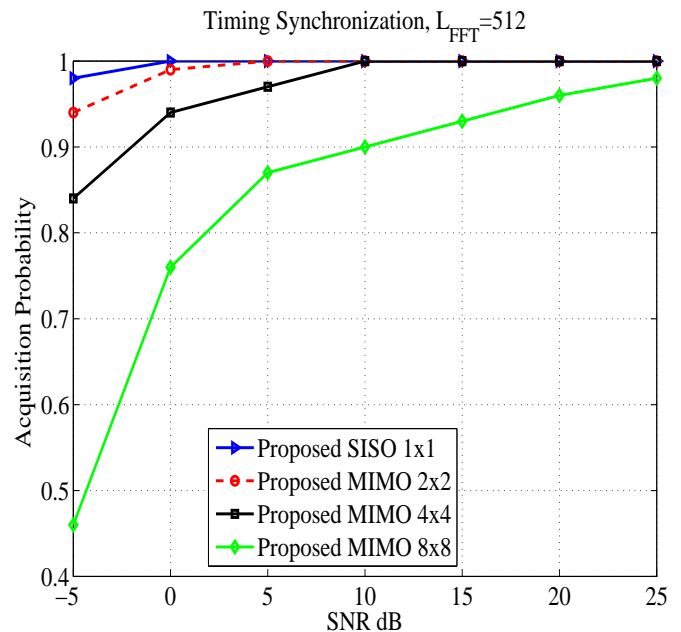


Fig. 15: Timing synchronization performance of the second proposed approach ($L_{FFT} = 512$)

E. Performance of our proposed approach

In this section, we present a comparison between our proposed approach, in order to find the most efficient among them. In the Figure 17, we obtained acquisition probability of our proposed approaches for MIMO-OFDM system 4×4 , and using the simulation parameters of Tables I and II.

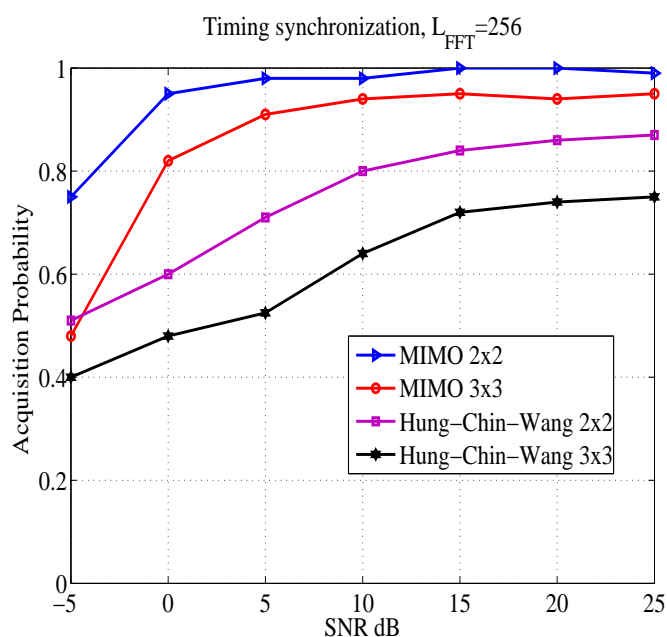


Fig. 16: Comparisons between the second proposed approach and subband-based preamble proposed in [23]

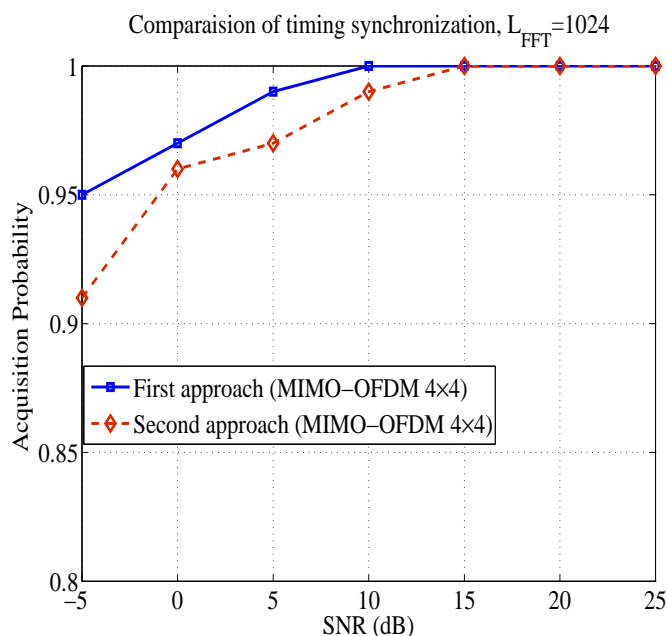


Fig. 17: Comparisons between the first and the second proposed approach for MIMO-OFDM system 4×4

The two approaches present a good timing synchronization acquisition probability at a low SNR. On the other hand, the acquisition probability of the first approach is perfect for an $SNR \geq 10$ dB, while its equal to 99% for the second approach for the same SNR. Therefore, the first approach presents a high performances versus the second approach. This performance is due to the good correlation function of the

synchronization preamble.

VII. CONCLUSION

One of the main challenges in a MIMO-OFDM system is the detection of the beginning of the received OFDM frames, this step called timing synchronization. The most of the timing synchronization methods are preamble based. In this paper, we proposed a novel compact preamble structure, in order to detect the timing frame synchronization. This structure is divided into two approaches. At the transmitter, a synchronization preamble is appended at the beginning of each OFDM frame. This preamble is based on CAZAC sequences, where those sequences have a good autocorrelation and cross-correlation functions.

At the receiver, and due to this combination, the correlation function between received signal and a local sequence shows a good frame detection with a large number of transmit antennas up to 8×8 . In comparison to the subband preamble based proposed by [23], our timing synchronization approaches present a better timing frame synchronization at a low SNR. Finally, we present the performance of our approaches, we find a few degradation of performance between our two approaches due to the correlation functions of different preambles structure. Our approaches can be implemented in MIMO-OFDM systems, with a large number of transmit antennas.

Even though there is still a large number of open research problems in the area of MIMO-OFDM systems. The proposed methods in this paper are presented for timing synchronization for such systems. Hence, it will be interesting to see the performance of our approach for frequency synchronization. Future work will assess, also, the performance of our approach in other communications systems.

ACKNOWLEDGMENT

This work was supported by the GET of Lebanese University and IETR of Rennes-France.

REFERENCES

- [1] A. Rachini, A. Beydoun, F. Nouvel, and B. Beydoun, "A novel compact preamble structure for timing synchronization in mimo-ofdm systems using cazac sequences," in International Conference on Communications, Computation, Networks and Technologies (INNOV), 2013, pp. 1–6.
- [2] IEEE Standard 802.11n: Wireless LAN Medium Access Control (MAC) and Physical Layer (PHY) Specifications Amendment 5: Enhancements for Higher Throughput, Institute of Electrical and Electronics Engineers, Oct. 2009.
- [3] R. Prasad, OFDM for Wireless Communications Systems. Norwood, MA, USA: Artech House, Inc., 2004.
- [4] B.R.Saltzberg and S.B.Weinstein, "Fourier transform communication systems," in Computer Machinery Conference, Pine Mountain, 1969.
- [5] A. Peled and A. Ruiz, "Frequency domain data transmission using reduced computational complexity algorithms," in Acoustics, Speech, and Signal Processing, IEEE International Conference on ICASSP '80., vol. 5, Apr. 1980, pp. 964–967.
- [6] D. Dromard and D. Seret, "Architecture des réseaux", 2nd ed. Pearson, Jun. 2013.
- [7] H. Jafarkhani, Space-Time Coding: Theory and Practice, 1st ed. New York, NY, USA: Cambridge University Press, 2010.

- [8] G. J. Foschini and M. J. Gans, "On limits of wireless communications in a fading environment when using multiple antennas," *Wireless Personal Communications*, vol. 6, 1998, pp. 311–335.
- [9] I. E. Telatar, "Capacity of multi-antenna gaussian channels," *European Transactions On Telecommunications*, vol. 10, no. 6, Dec. 1999, pp. 585–595.
- [10] S. Alamouti, "A simple transmit diversity technique for wireless communications," vol. 16, no. 8, Oct. 1998, pp. 1451–1458.
- [11] V. Tarokh, N. Seshadri, and A. Calderbank, "Space-time codes for high data rate wireless communication: performance criterion and code construction," *Information Theory, IEEE Transactions on*, vol. 44, no. 2, 1998, pp. 744–765.
- [12] V. Tarokh, A. Naguib, N. Seshadri, and A. Calderbank, "Space-time codes for high data rate wireless communication: performance criteria in the presence of channel estimation errors, mobility, and multiple paths," *Communications, IEEE Transactions on*, vol. 47, no. 2, Feb. 1999, pp. 199–207.
- [13] T. Schmidl and D. Cox, "Robust frequency and timing synchronization for ofdm," *Communications, IEEE Transactions on*, vol. 45, no. 12, Dec. 1997, pp. 1613–1621.
- [14] U. Rohrs and L. Linde, "Some unique properties and applications of perfect squares minimum phase cazac sequences," in *Communications and Signal Processing, 1992. COMSIG '92., Proceedings of the 1992 South African Symposium on*, Sept. 1992, pp. 155–160.
- [15] B. Yang, K. Letaief, R. Cheng, and Z. Cao, "Burst frame synchronization for ofdm transmission in multipath fading links," in *Vehicular Technology Conference, 1999. VTC 1999 - Fall. IEEE VTS 50th*, vol. 1, 1999, pp. 300–304 vol.1.
- [16] J.-J. van de Beek, M. Sandell, M. Isaksson, and P. Ola Borjesson, "Low-complex frame synchronization in ofdm systems," in *Universal Personal Communications. 1995. Record., 1995 Fourth IEEE International Conference on*, Nov. 1995, pp. 982–986.
- [17] L. Li and P. Zhou, "Synchronization for b3g mimo ofdm in dl initial acquisition by cazac sequence," in *Communications, Circuits and Systems Proceedings, 2006 International Conference on*, vol. 2, Jun. 2006, pp. 1035–1039.
- [18] R. Frank, S. Zadoff, and R. Heimiller, "Phase shift pulse codes with good periodic correlation properties (corresp.)," *Information Theory, IRE Transactions on*, vol. 8, no. 6, Oct. 1962, pp. 381–382.
- [19] V. Tarokh, H. Jafarkhani, and A. Calderbank, "Space-time block codes from orthogonal designs," *Information Theory, IEEE Transactions on*, vol. 45, no. 5, 1999, pp. 1456–1467.
- [20] A. Rachini, A. Beydoun, F. Nouvel, and B. Beydoun, "Timing synchronisation method for mimo-ofdm system using orthogonal preamble," in *Telecommunications (ICT), 2012 19th International Conference on*, 2012, pp. 1–5.
- [21] W. Jian, L. Jianguo, and D. Li, "Synchronization for mimo ofdm systems with loosely synchronous (ls) codes," in *Wireless Communications, Networking and Mobile Computing, 2007. WiCom 2007. International Conference on*, Sept. 2007, pp. 254–258.
- [22] G. Gaurshetti and S. Khobragade, "Orthogonal cyclic prefix for time synchronization in mimo-ofdm," *International Journal of Advanced Electrical and Electronics Engineering (IJAEED)*, vol. 2, 2013, pp. 81–85.
- [23] H.-C. Wang and C.-L. Wang, "A compact preamble design for synchronization in distributed mimo ofdm systems," in *Vehicular Technology Conference (VTC Fall), 2011 IEEE*, Sept. 2011, pp. 1–4.
- [24] R. Gold, "Optimal binary sequences for spread spectrum multiplexing (corresp.)," *Information Theory, IEEE Transactions on*, vol. 13, no. 4, Oct. 1967, pp. 619–621.
- [25] J. G. Proakis, *Digital Communications*, 4th ed. McGraw-Hill, 2000.
- [26] R. Frank, S. Zadoff, and R. Heimiller, "Phase shift pulse codes with good periodic correlation properties (corresp.)," *Information Theory, IRE Transactions on*, vol. 8, no. 6, Oct. 1962, pp. 381–382.
- [27] P. Fan and M. Darnell, *Sequence Design for Communications Applications*. John Wiley & Sons Ltd., 1996.
- [28] B. O'Hara and A. Petrick, *The IEEE 802.11 Handbook: A Designer's Companion*. Standards Information Network IEEE Press, 1999.